Exp Brain Res (1990) 82:519–535

Experimental Brain Research

$GABA_A$ receptor immunoreactivity in adult and developing monkey sensory-motor cortex

G.W. Huntley[1], A.L. de Blas[2]*, and E.G. Jones[1]

[1] Department of Anatomy and Neurobiology, University of California, Irvine, CA 92717, USA
[2] Department of Neurobiology and Behaviour, State University of New York, Stony Brook, NY 11794, USA

Received February 26, 1990 / Accepted June 1, 1990

Summary. The areal and laminar distribution of $GABA_A$ receptor immunoreactivity was examined in fetal, early postnatal and adult monkey sensory-motor cortex by using a monoclonal antibody to the purified $GABA_A$ receptor complex (Vitorica et al. 1988). $GABA_A$ receptor immunoreactivity was distributed throughout the neuropil, often outlining the unstained somata of pyramidal and non-pyramidal cells. In all areas of the adult sensory-motor cortex, layers I–IIIA exhibited the most intense immunostaining. In deeper layers of the four cytoarchitectonic fields of the first somatic sensory area (SI), layers IIIB and V were lightly stained and alternated with somewhat more intensely stained layers IV and VI. In deeper layers of area 4, the deeper half of layer IIIA through layer VA was lightly immunostained, but layers VB and VI were slightly more intensely immunoreactive. A variable number of nonpyramidal cell somata in the cortex and underlying white matter showed immunoreactive staining. $GABA_A$ receptor immunoreactivity was present throughout the sensory-motor cortex from the youngest fetal age examined (E121), but the pattern of immunostaining differed from that in the adult. In all areas, the densest immunoreactivity was found in a diffuse band in layers III and IV and in the subplate zone. Within the subplate zone, the presence of receptor immunoreactivity and some intensely stained neuronal somata at all fetal ages suggests the presence of a synaptic neuropil. With increasing age, gradual changes in the distribution of receptor immunoreactivity occurred, resulting in an adult-like pattern of immunostaining by postnatal day 1.5. These results show that the laminar pattern of $GABA_A$ receptor distribution closely follows the major concentrations of GABA immunoreactive neurons in adults and it is suggested that laminar changes seen in development are associated with the establishment of afferent connections and inhibitory circuits in the sensory-motor cortex.

* Present address: Division of Molecular Biology, University of Missouri-Kansas City, Kansas City, MO 64110, USA

Offprint requests to: E.G. Jones (address see above)

Key words: GABA – Receptors – Immunocytochemistry – Inhibitory circuitry – Cortical development – Primate

Introduction

The functional properties of many neocortical neurons are determined to a large extent by inhibitory mechanisms (Creutzfeld and Ito 1968; Tsumoto et al. 1979; Hicks and Dykes 1983; Dykes et al. 1984; Sillito 1984; Alloway and Burton 1986; Ramoa et al. 1988; Juliano et al. 1989), which in turn are thought to derive from a specific subset of cortical interneurons that release the neurotransmitter gamma aminobutyric acid (GABA) (Houser et al. 1984). The importance of GABA-mediated inhibition in cortical function has generated considerable interest in the synaptic organization of GABAergic cells and the distribution of the receptors thought to mediate GABAergic inhibitory activity.

Two GABA receptor subtypes, $GABA_A$ and $GABA_B$, have been identified (Bowery et al. 1984; Enna 1988). The $GABA_A$ receptor is a complex thought responsible for the major form of neocortical inhibitory postsynaptic potential: that which arises from an increase in chloride conductance (Kelly et al. 1969; Connors et al. 1988). In addition to being coupled to a chloride channel, the $GABA_A$ receptor includes at least five binding sites, among which are those for benzodiazepines and barbiturates (Barnard et al. 1987).

In the somatic sensory cortex, the functional role of $GABA_A$ receptor-mediated inhibition has been studied with bicuculline methiodide (BIC), a competitive $GABA_A$ receptor antagonist. Iontophoretic application of BIC to the somatic sensory cortex of cats causes an increase in the response magnitude to a given stimulus and an expansion of the receptive field size for certain classes of neurons (Hicks and Dykes 1983; Dykes et al. 1984; Alloway and Burton 1986). Additionally, certain cells which previously could not be driven by somatic

stimulation, exhibit cutaneous receptive fields following BIC application (Dykes et al. 1984).

In adult monkey sensory-motor cortex, the distribution and synaptic organization of GABAergic cells and terminals have been studied autoradiographically following the uptake of ^{3}H–GABA (Hendry and Jones 1981; DeFelipe and Jones 1985) and by GABA or glutamic acid decarboxylase (GAD) immunocytochemistry (Hendry et al. 1983, 1987b; Houser et al. 1983; DeFelipe et al. 1986; Chudler et al. 1988). Studies of the developing monkey sensory-motor cortex indicate that many GABA-immunoreactive cells and processes are present from very early stages (Huntley et al. 1987; Huntley and Jones 1990), but the development of the $GABA_A$ receptor has not been examined. In adult monkey sensory-motor cortex, quantitative receptor autoradiography has been utilized to describe the areal and laminar distribution of $GABA_A$ and benzodiazepine receptors (Lidow et al. 1990). In the present study of the developing and adult sensory-motor areas, advantage has been taken of the greater resolution afforded by immunocytochemical techniques to provide a more detailed analysis of the laminar and cellular distribution of $GABA_A$ receptors in the sensory-motor areas than that available from receptor autoradiography, and to document the changes occurring in the course of late fetal and early postnatal development and leading up to the adult pattern.

Material and methods

Tissue preparation

This study was carried out on the sensory-motor areas from four normal adult macaque monkeys (two *Macaca fascicularis,* one *Macaca nemestrina* and one *Macaca mulatta*), six fetal monkeys (one *Macaca nemestrina,* aged 125 days post-conception, (E125) and five *Macaca mulatta* aged E121, E131, E135, E150 and E155), and six early postnatal monkeys (five *Macaca nemestrina*, aged 1.5, 21, 60, 120 and 125 postnatal days (PND), and one *Macaca mulatta,* aged 77PND). The adult monkeys, some of which had been used in other studies (Hendry et al. 1990), were given an overdose of Nembutal and perfused through the heart with 4% paraformaldehyde and 0.02–0.05% glutaraldehyde in 0.1 M phosphate buffer. The fetal rhesus monkeys, all of which had also been used in other studies (Chalupa and Killackey 1987; Hendry et al. 1987a; Huntley et al. 1987, 1988; Huntley and Jones 1990), were deeply anesthetized and perfused transcardially with normal saline followed by 2% paraformaldehyde and 0.1% glutaraldehyde in 0.1 M phosphate buffer. The fetal and infant pig-tailed monkeys were deeply anesthetized and perfused transcardially first with 5% dextrose in Ringer's solution which contained 2% heparin, followed by 4% paraformaldehyde and 0.1% glutaraldehyde in 0.1 M phosphate buffer. This was followed by 5% dextrose-Ringer's solution and then by 20% sucrose. The infant rhesus monkey was deeply anesthetized and perfused first with cold 1% paraformaldehyde followed by cold 4% paraformaldehyde in 0.1 M PO_4 buffer. All brains, after removal, were subsequently removed, blocked, infiltrated with 30% sucrose and frozen on dry ice.

Immunocytochemistry and histochemistry

Frozen sections were cut at 20 μm on a freezing microtome in either the frontal or sagittal plane, or, from blocks flattened prior to freezing, in a plane parallel to the pial surface. One series of sections from each block was preincubated in a solution containing 5% normal horse serum and 0.25% Triton X–100 in 0.1 M phosphate buffer for five h at 4° C, then transferred to an identical solution which contained in addition a monoclonal antibody to the $GABA_A$ receptor (62–3G1, diluted 1:250; de Blas et al. 1988; Vitorica et al. 1988). Following incubation for 48 h at 4° C, the sections were processed by the avidin-biotin-peroxidase method using Vectastain Kits (Vector Labs), and reacted with 3,3' diaminobenzidine tetrahydrochloride (20 mg/100 ml 0.1 M phosphate buffer). The sections were mounted on gelatin-coated slides, dehydrated and coverslipped.

Areal and laminar boundaries were determined from separate series of sections either stained with thionin or processed histochemically for cytochrome oxidase activity (Wong-Riley 1979) or acetylcholinesterase activity (Woolf and Butcher 1981).

No specific staining occurred in control sections in which the primary antibody was replaced by normal mouse serum or supernatant from a non-secreting cell line, each at approximately twice the concentration of the primary antibody solution.

Densitometry

The laminar intensity of receptor immunostaining was assessed using an MCID image analysis system. Relative optical density measurements from a series of ten separate samples were taken from each layer of cortex, and statistically significant differences in intensity across layers from single sections were determined using a two-tailed t-test.

Results

$GABA_A$ receptor immunoreactivity in the adult sensory-motor cortex

Immunoreactivity for the $GABA_A$ receptor was present in all layers of the first somatic sensory cortex (SI; areas 3a, 3b, 1 and 2) and of the primary motor cortex (area 4) (Figs. 1, 2, 5). There were no qualitative differences in laminar distribution or relative intensity of immunostaining between the three species of macaques examined. In each of the areas examined, immunoreactivity was distributed throughout the neuropil; the reaction product appeared finely granular with interspersed large, dark punctate profiles (Fig. 2). Concentrations of homogeneous staining or puncta often outlined the somata of unstained pyramidal and non-pyramidal neurons (Fig. 2). In addition to neuropil immunostaining, each of the areas examined possessed variable numbers of cells whose somata and proximal processes were immunoreactive (see below).

Area 4

The density of $GABA_A$ receptor immunostaining varied across laminae in the motor cortex (Fig. 1C). Neuropil staining was distributed fairly evenly within a lamina, and often outlined the unstained somata of pyramidal and round or ovoid non-pyramidal cells.

Dense neuropil staining was present in layers I, II and the upper half of layer IIIA (Fig. 1C). The deeper part of layer IIIA through layer VA was lightly stained rela-

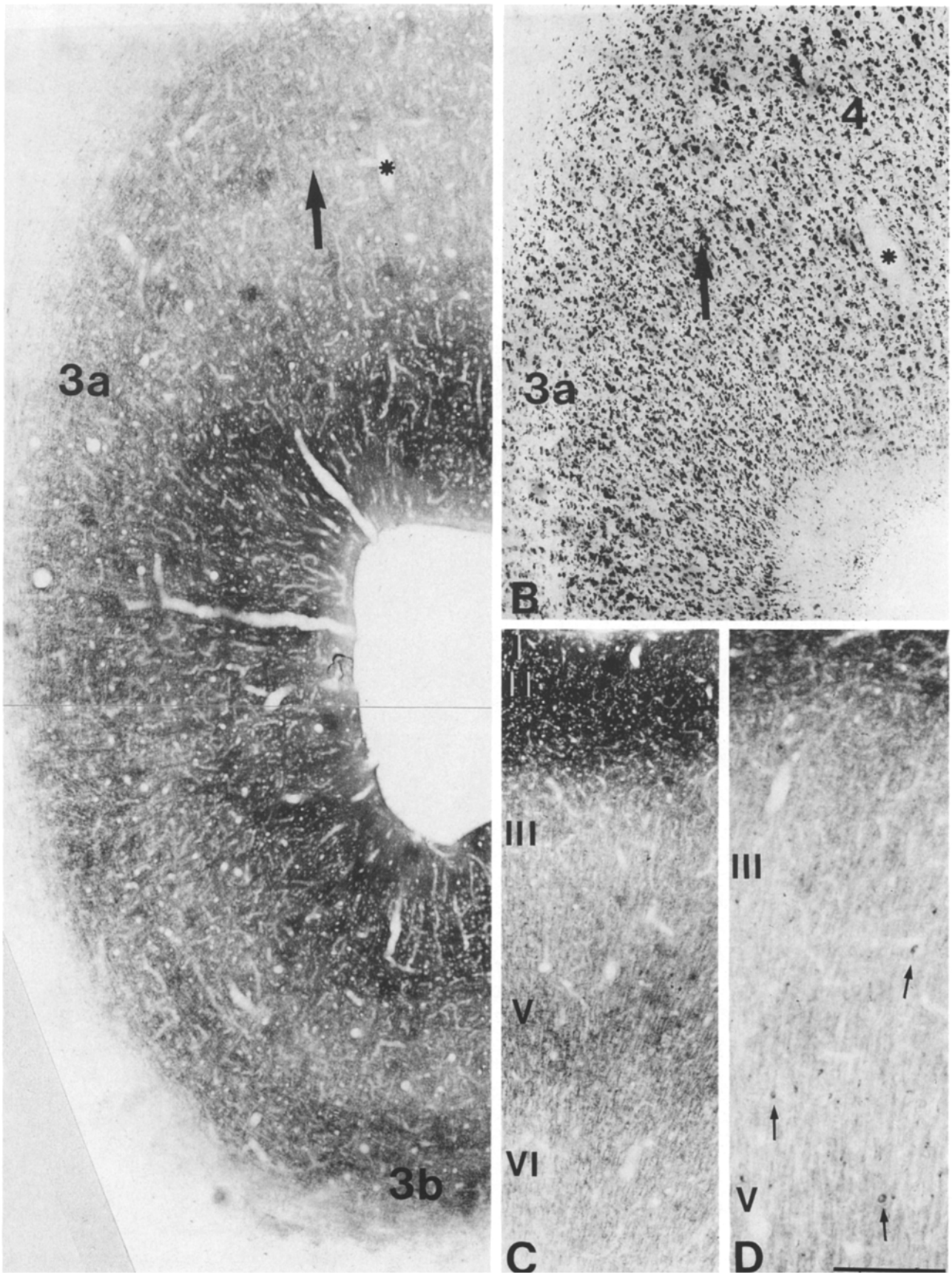

Fig. 1A–D. Photomicrographs of sagittal sections through the sensory-motor cortex of an adult monkey stained immunocytochemically for $GABA_A$ receptors (**A, C, D**) or stained with thionin (**B**). The pattern of immunostaining is similar throughout areas 3a and 3b, but changes at the area 3a/4 border (*arrows* in **A, B**). The asterisk in **A, B** denotes the same blood vessel. **C** Area 4. The greatest intensity of immunostaining occurs in layers I–IIIA, with a less intense band in layers VB–VIA. **D** Area 4. Numerous stained non-pyramidal somata *(arrows)*, and long, parallel streaks of receptor immunoreactivity are present. Numbers in this and subsequent figures refer to cytoarchitectonic areas. Roman numerals refer to layers of the cortex. Bar: 300 μm (**A, B**), 400 μm (**C**) or 200 μm (**C**)

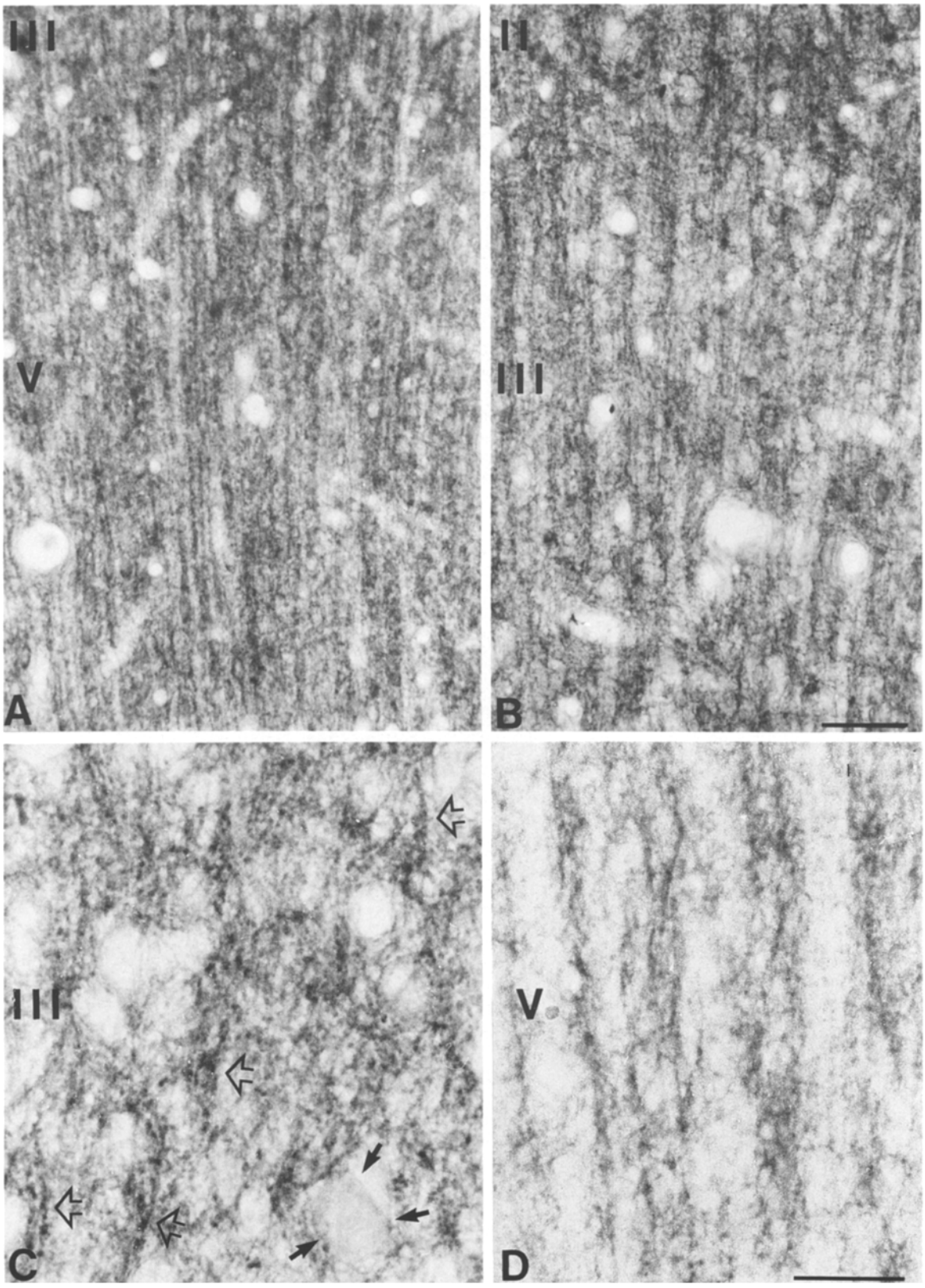

Fig. 2A–D. Photomicrographs of $GABA_A$ receptor immunoreactive sections through area 4 (**A**) and area 1 (**B–D**). Parallel chains of densely-stained puncta are present in superficial layers (shown at higher power by open arrows in **C**). In middle and deep layers, long streaks of staining resembling radial fasciculi are evident (shown at higher power in **D**). Solid arrows in **C** show an unstained neuron outlined by immunoreactivity. Bar in B, 50 μm (**A**) or 40 μm (**B**); bar in **D**, 6 μm (**C, D**)

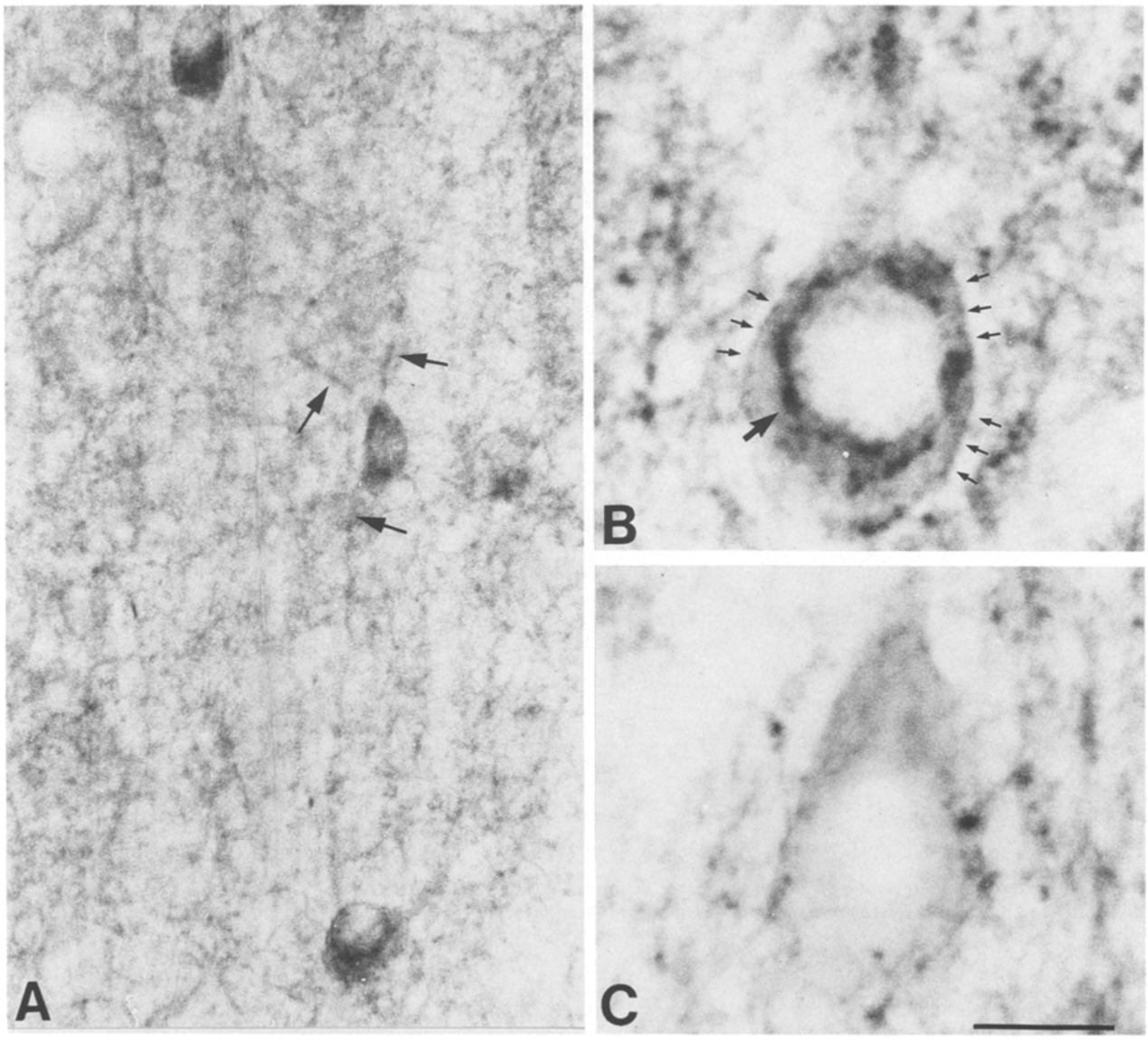

Fig. 3A–C. $GABA_A$ receptor immunoreactive cells in area 4 of an adult monkey. **A** Stained proximal processes *(arrows)* of small immunoreactive somata reveal multipolar, non-pyramidal morphology. **B** Higher-power photomicrograph showing cellular distribution of reaction product around cell membrane *(small arrows)* and concentrated in puncta or patches on or within the cell *(large arrow)*. **C** Giant pyramidal cell of layer V. The cell membrane appears lightly immunoreactive. Bar: 30 μm (**A**), 12 μm (**B**), 20 μm (**C**)

tive to superficial layers ($p < 0.0005$). Layer VB through the upper half of layer VI was more intensely stained than layer IIIB–VA ($p < 0.005$), but was less densely stained than layers I–IIIA ($p < 0.0005$) (Fig. 1C). Commonly, parallel chains of densely stained puncta resembling small fasciculi descended vertically through layer IIIA before becoming lost in layer IIIB (Figs. 1D, 2A). The receptor immunoreactivity throughout layers III–VI also showed evidence of long streaks of staining, less punctate than the chains in layer IIIB, and alternating with clear spaces, or spaces with only very light immunostaining (Figs. 1D, 2A). These streaks of staining descended into the white matter and had a periodicity resembling that of the radial fasciculi of the cortex.

Layers IIIA–V possessed a moderate number of cell somata and their proximal processes that were immunoreactive (Figs. 1D, 3). The majority of such cells were small, although occasional larger somata were also stained. When processes were stained, the cells appeared as multipolar non-pyramidal neurons (Fig. 3A). The processes could not be followed for more than a few tens of microns from their somata of origin. In general, the immunoreactivity was strongest along the cell membrane, but was also concentrated in the perinuclear cytoplasm and occasionally small patches of staining were present in other parts of the cytoplasm (Fig. 3B). The cell membranes of the giant pyramids of layer V were very lightly and evenly stained (Fig. 3C). Very occasional immunoreactive cell somata were present in layers II and VI, but none were present in layer I. The density of the immunoreactivity in these layers obscured any selective staining of cell membranes.

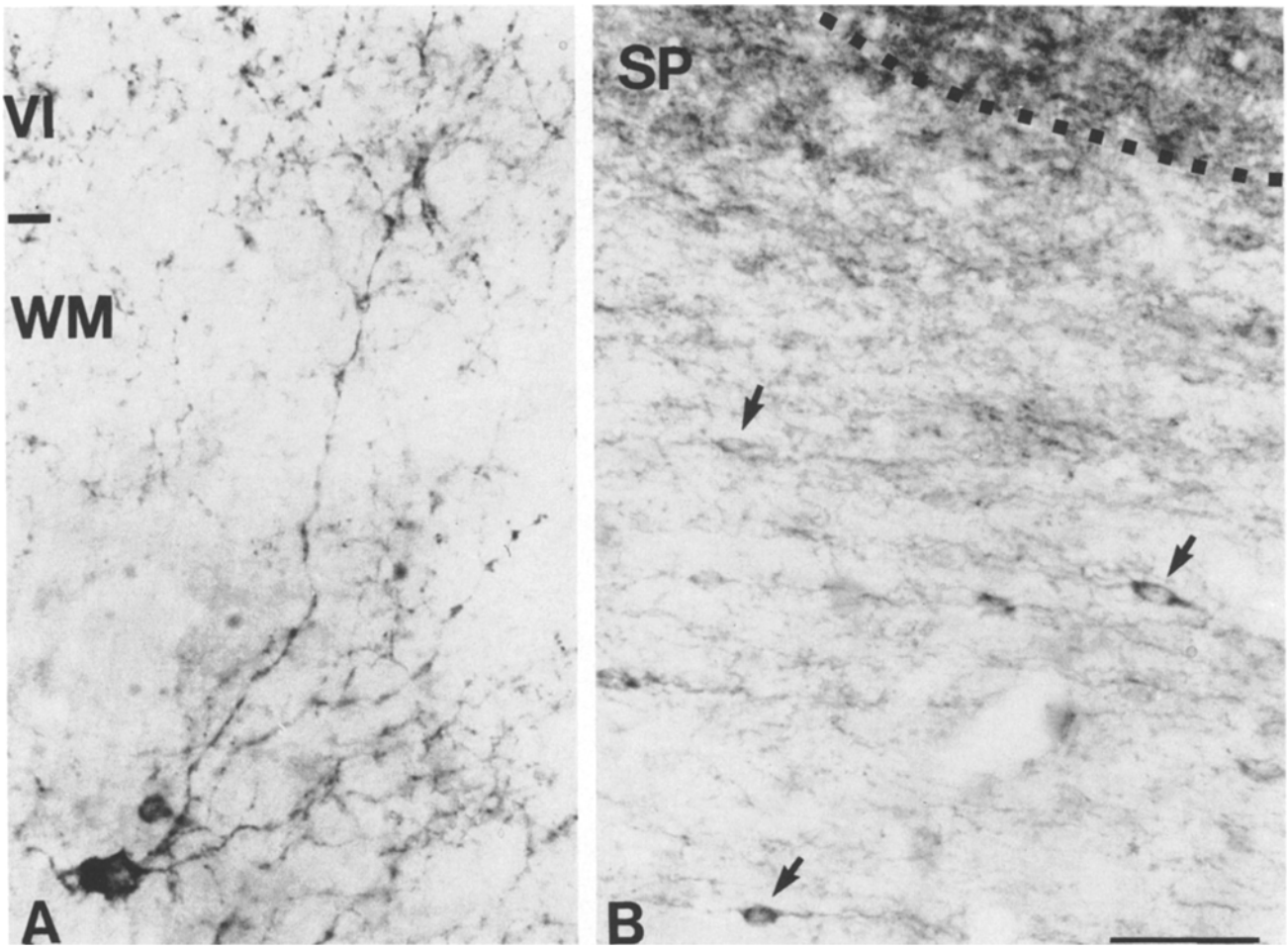

Fig. 4. **A** Immunostained cell in white matter (WM) beneath layer VI in area 4 of an adult animal. **B** Subplate immunoreactive cells *(arrows)* from a fetal monkey (E135). Dotted line represents the separation between layer VI (above line) and the subplate (SP). Bar: 35 μm (**A**), 45 μm (**B**)

In the underlying white matter there were sparsely distributed, immunostained ovoid somata, many of which sent long, thin processes into the overlying cortex (Fig. 4A). The immunoreactivity was strongest around the edges of such cells, suggesting localization to the cell membrane, but light, diffuse immunoreactivity was also present intracellularly.

Area 3

In areas 3a and 3b, moderate neuropil staining was present in layer I, but layer II and the upper half of layer III were intensely stained (Figs. 1A, 5). The deeper half of layer III (IIIB) and layer V were similar to each other in intensity of staining, and were more lightly immunoreactive ($p < 0.0005$). Layers IV and VI showed enhanced immunoreactive staining relative to layers IIIB and V ($p < 0.05$), but the density did not approach that of layers II and IIIA. There were no differences in the pattern of $GABA_A$ receptor immunostaining between areas 3a and 3b (Fig. 1A). The staining of layer IV formed a continuous stratum through both areas.

In the deeper half of layer III, short, radially-oriented segments of clustered immunoreactivity similar to those in area 4 were present (Fig. 5A). However, in contrast to area 4, receptor immunoreactivity in the deeper layers was less distinctly clustered into long, radially-oriented streaks (Figs. 1A, 5A). Instead, the receptor immunoreactivity appeared more evenly distributed throughout the neuropil.

There were fewer immunoreactive somata in areas 3a and 3b than in area 4, both within the cortex and in the underlying white matter. Stained cells present in the cortex were small, non-pyramidal cells distributed in the middle layers. The white matter cells were similar to those beneath area 4.

The anterior border of area 3a was not particularly sharp, but could be detected by the disappearance of the immunoreactive band corresponding to layer IV of area 3a on passing into area 4 (Fig. 1A, B).

Areas 1 and 2

There were no overt changes in the laminar distribution or intensity of receptor immunostaining in passing from area 3b caudally into area 1, or between areas 1 and 2

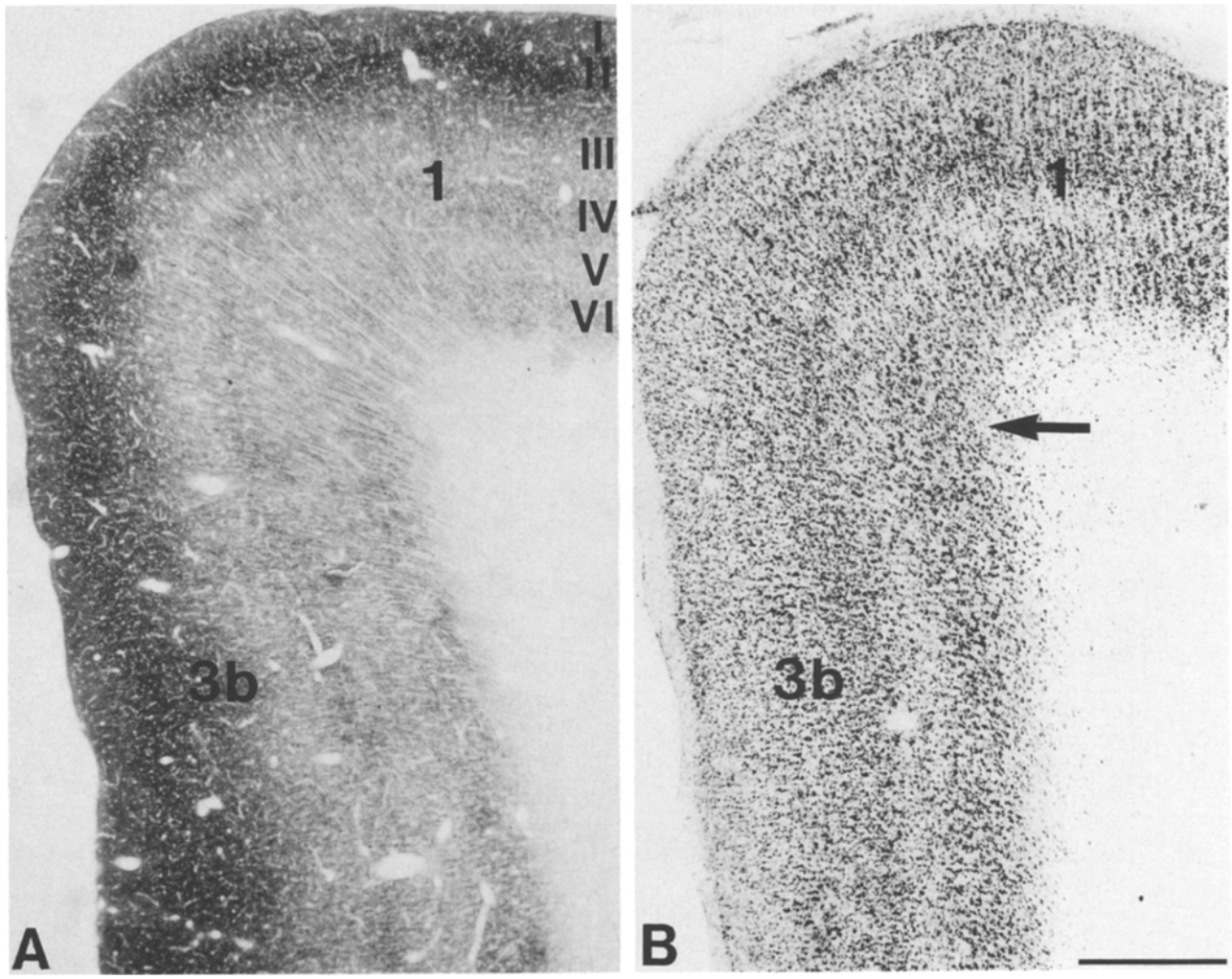

Fig. 5A, B. Photomicrographs of sagittal sections through the postcentral gyrus of an adult monkey and stained immunocytochemically for $GABA_A$ receptors (**A**) or with thionin (**B**). Each of the areas of SI shows a similar pattern of immunostaining, with no differences in intensity or distribution apparent at the border between areas 3b and 1 (*arrow* in **B**). Bar: 670 μm (**A**), 570 μm (**B**)

(Fig. 5). The layer IV stratum, for example, passed continuously from area 3 into area 1 and the dense staining in layers II and III showed no change in intensity or superficial to deep extent at the border (Fig. 5). In contrast to areas 3a and 3b, however, receptor immunoreactivity, particularly in area 1, was strongly organized into long, vertically-oriented chains spanning upper layer III and with strong radial streaks extending from layer III into the white matter (Figs. 2B, C, D; 5).

In both areas, immunoreactive somata similar to those already described were present, their density resembling that seen in and beneath areas 3a and 3b.

$GABA_A$ receptor immunoreactivity in the developing sensory-motor cortex

Immunoreactivity for the $GABA_A$ receptor was present throughout the pre- and postcentral gyri at each of the fetal and early postnatal ages examined, but exhibited changes in laminar distribution and intensity over time (Fig. 6).

At the youngest fetal ages examined (E121 and E125), in Nissl stained sections both the presumptive motor and first somatic sensory areas are composed of six, clearly delineated cellular layers. Only the border between areas 3a and 4 can be detected at this age (Fig. 7); the characteristic cytoarchitectonic borders in the postcentral gyrus resolve themselves between E121 and E135 (unpublished observations).

The patterns of $GABA_A$ receptor immunostaining at E121 and E125 were similar, and are described together. Overall, receptor immunoreactivity throughout the sensory-motor areas showed a continuous and mostly similar pattern of distribution. In all areas, layers I and II were lightly immunostained (Fig. 7A, C). A more intense, though diffuse band of immunoreactivity was present throughout the neuropil of layers III and IV ($p < 0.0005$) (Figs. 7A, C) The staining intensity of the band corresponding to layers III and IV of the postcentral gyrus decreased somewhat at the area 3a/4 border (Fig. 7B).

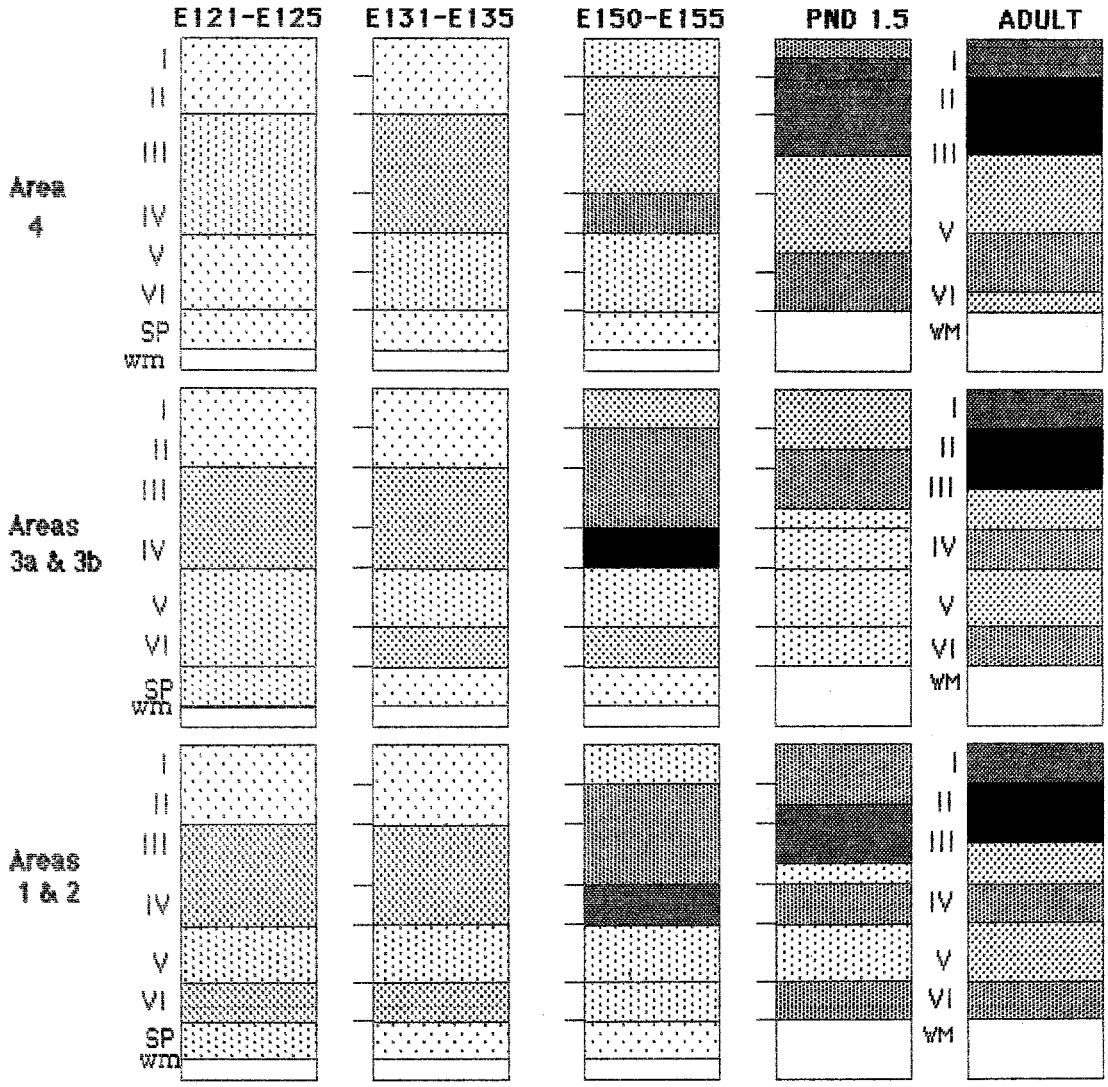

Fig. 6. Schematic diagram illustrating the major changes in laminar distribution and staining intensity of receptor immunoreactivity in areas 4, 3a, 3b,1 and 2 from E125 to adulthood. Increasing density of stippling represents increasing intensity of the immunostaining. Note that the laminar boundaries depicted are schematic, and are not meant to reflect accurately changes in laminar thickness with increasing age

Layer V was more lightly stained than layer IV throughout all areas ($p < 0.005$), and was similar in intensity to that of layer VI in areas 4, 3a and 3b (Figs. 6, 7A). However, on passing caudally there appeared on the crown of the postcentral gyrus a more intensely stained band corresponding to layer VI which remained throughout areas 1 and 2 (Fig. 7A, C). Underlying layer VI of all regions was a diffuse band of punctate immunoreactivity which likely corresponds to the subplate region (Fig. 7A, C). The thickness of the subplate staining was at E121 and E125 greater on the convexity of the pre- and postcentral gyri, and became gradually thinner along both banks and in the fundus of the central sulcus beneath area 3a. Deep to the band of subplate staining, the white matter became free of immunostaining ($p < 0.0005$) (Fig. 7A).

In contrast to the adult pattern, the cortical immunoreactivity in any area examined lacked overt vertical clustering or streaking, but appeared more fenestrated on account of the closely spaced holes corresponding to the somata of neurons (Fig. 7C). There were no immunoreactive somata present within the cortex, although immunoreactivity outlined the somata of many, otherwise unstained cells. There were small numbers of immunostained somata present in the subplate. These were characterized by ovoid somata commonly aligned parallel to the overlying cortex or fiber fasciculi of the white matter, and they commonly had long slender processes emerging from each pole (Fig. 4B).

The adult laminar pattern of $GABA_A$ receptor immunoreactivity was gradually acquired in the course of late fetal and early postnatal development (Fig. 6). At E131 and E135, the overall laminar distribution of immunoreactivity was similar to that at the earlier ages examined in each area (Fig. 6). However, layer VI in areas 3a and 3b was more intensely stained than at the younger ages examined, and appeared as a homogeneous band throughout the postcentral gyrus (Fig. 6). The diffuse receptor immunoreactivity in the subplate described at younger ages had mostly disappeared by E135, although

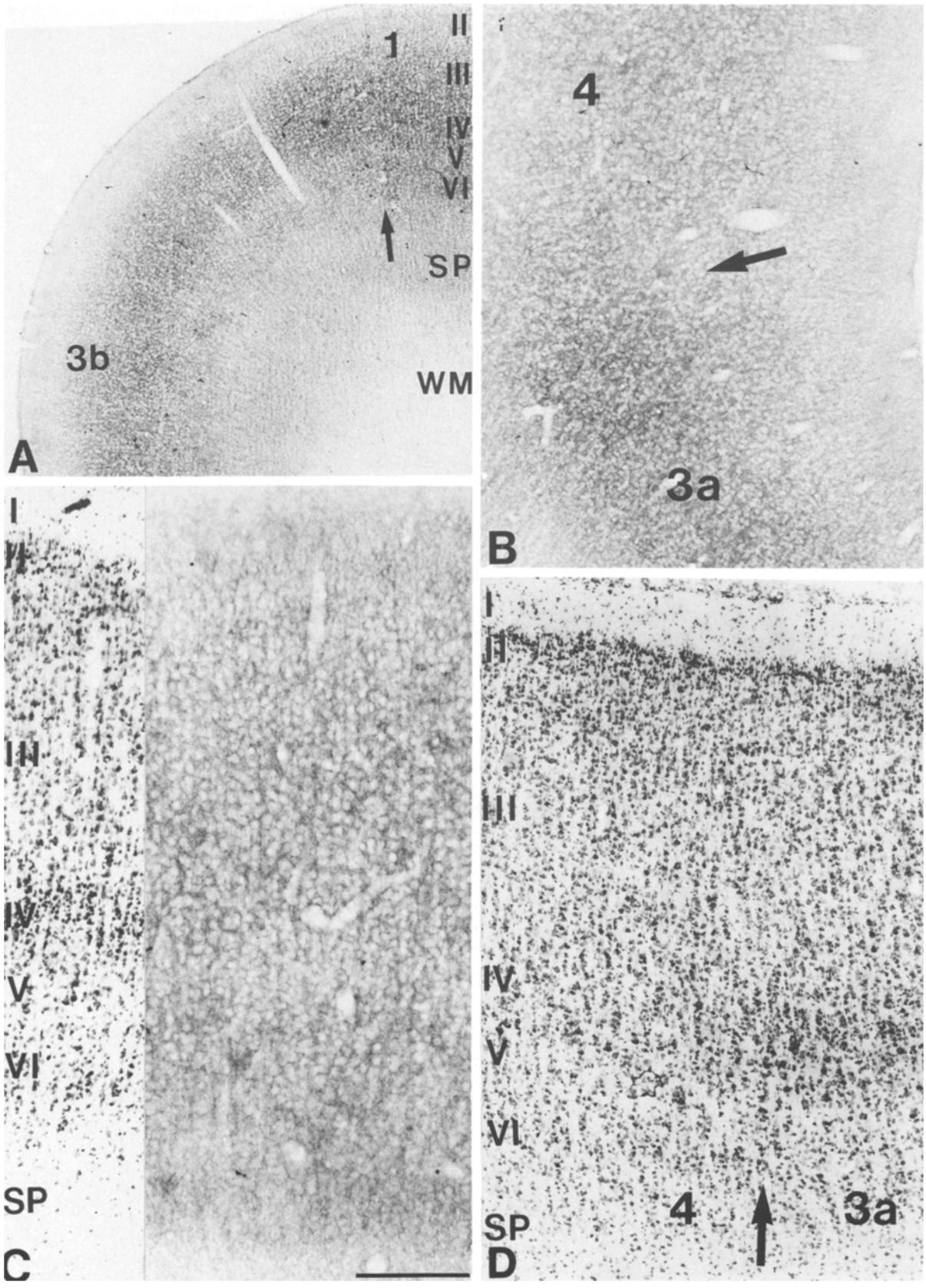

Fig. 7A–D. Photomicrographs of sections taken from an E125 fetal monkey. **A** Distribution of $GABA_A$ receptor immunoreactivity across areas of the postcentral gyrus and in the subplate zone (SP). Arrow indicates position at which the intensity of immunostaining in layer VI increases on crown of postcentral gyrus and remains throughout the exposed part of the gyrus; a higher power photomicrograph of this is shown through area 2 in **C**. **B** Differences in intensity of immunostaining demarcates the border between areas 3a and 4 *(arrow)*; the cytoarchitectonic border is shown in thionin stained section **D**. Bar: 500 μm (**A**), 300 μm (**B**), 235 μm (**C**), 285 μm (**D**)

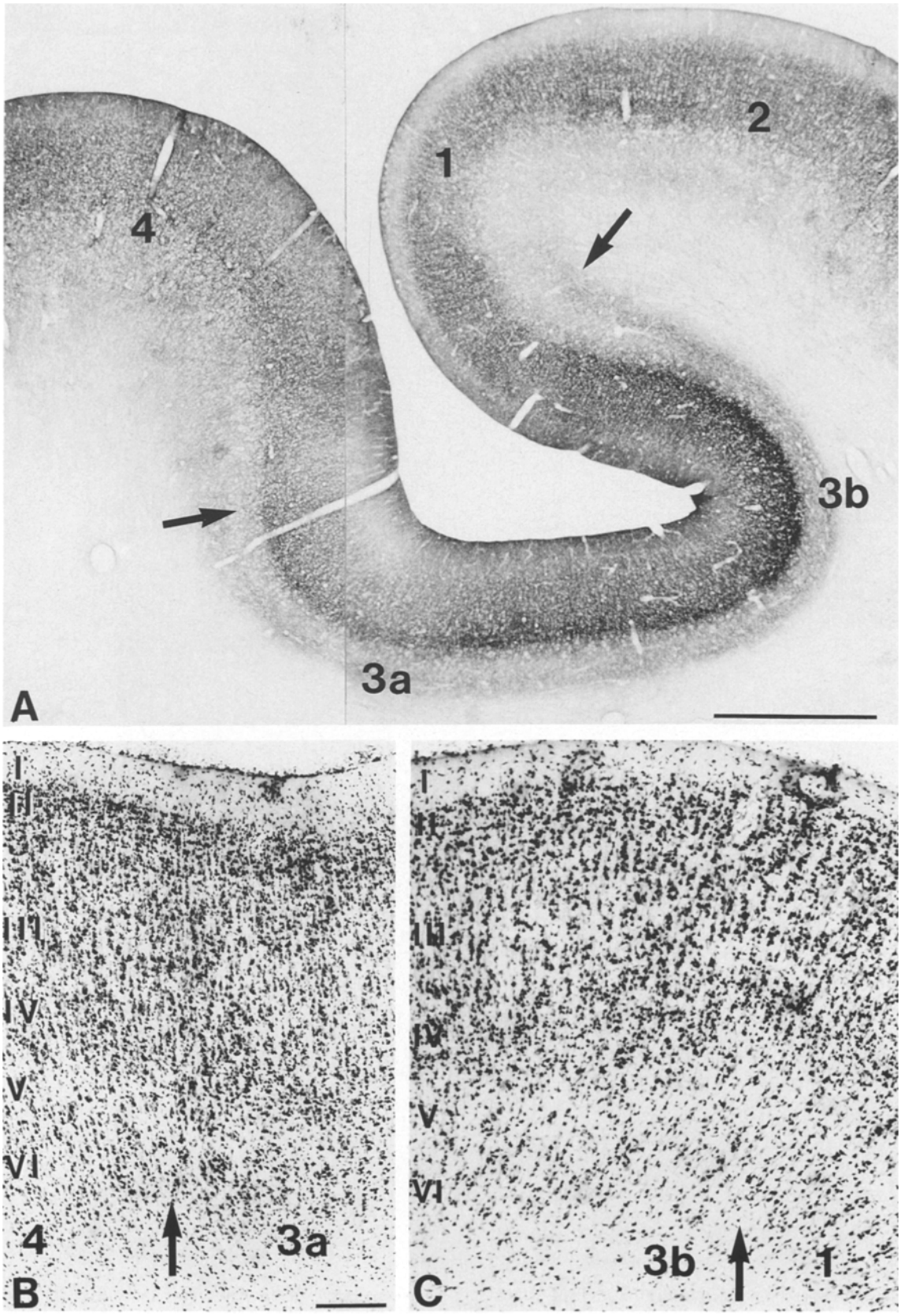

Fig. 8A–C. Photomicrographs of sections through the sensory-motor cortex of an E155 fetal monkey stained for $GABA_A$ receptor immunoreactivity (**A**) or with thionin (**B, C**). Immunoreactivity at this stage demarcates the area 3a/4 border (*left arrow* in **A**), shown at higher power in B, and the area 3b/1 border (*right arrow* in **A**), shown at higher power in **C**. Bar: 1 mm (**A**); 200 μm (**B**) or 150 μm (**C**)

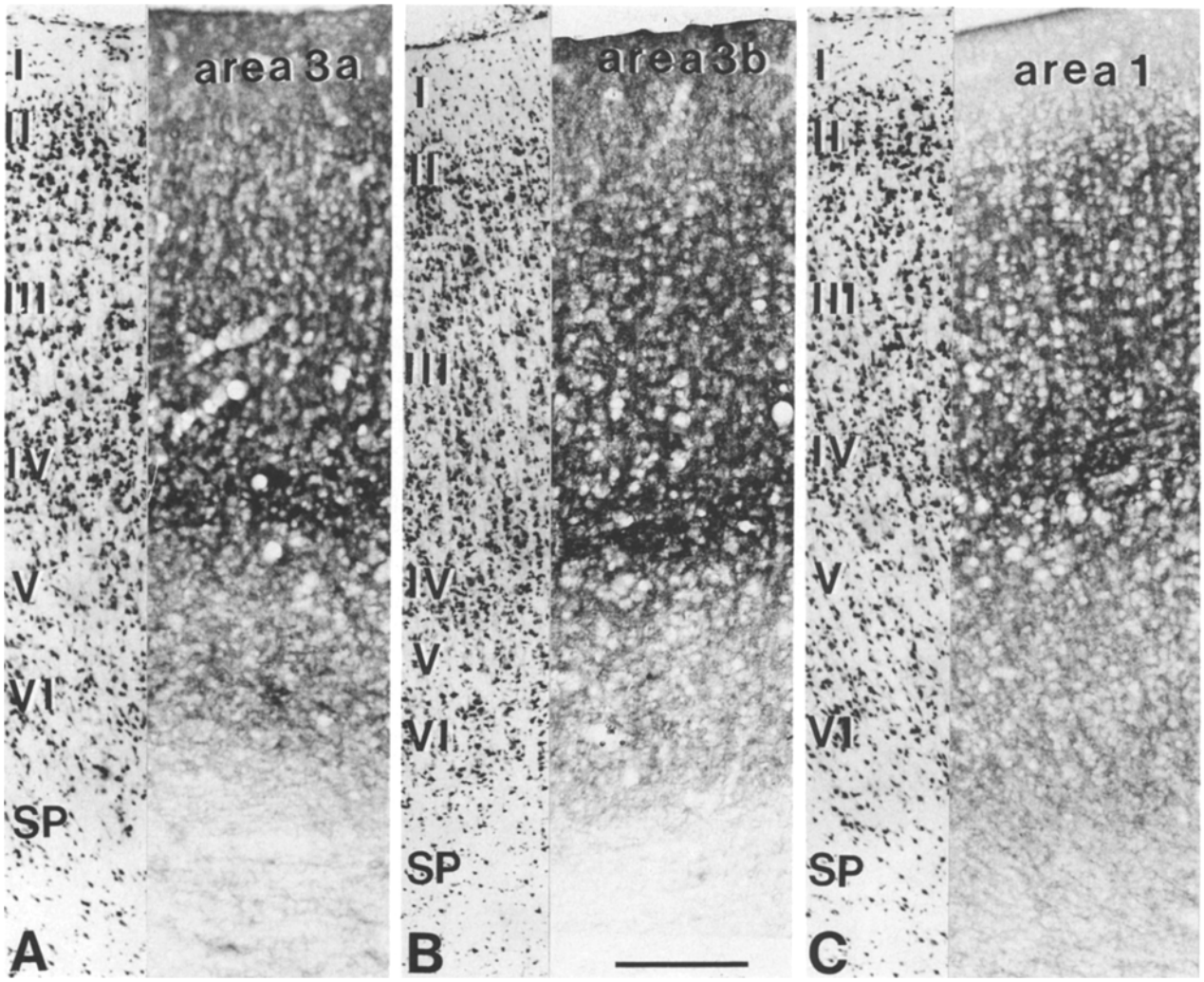

Fig. 9A–C. Pairs of photomicrographs from adjacent sections stained with thionin or for $GABA_A$ receptor immunoreactivity through area 3a (**A**), area 3b (**B**) or area 1 (**C**) from an E155 fetal monkey, demonstrating laminar distribution and intensity of immunostaining at this stage. SP = subplate. Bar: 150 μm

a few bipolar and tripolar stained cells were still present.

The staining intensity, overall, at E150 and 155 was greater than at previous ages, but staining was greatest in layer IV throughout areas 3a and 3b (Figs. 6, 8, 9). The anterior border of area 3a was clearly demarcated by the greater intensity of layer IV immunostaining which decreased in intensity and continued as a thin, less intensely stained band through the transient layer IV still present in the motor cortex at this stage (Fig. 8A, B). Posteriorly, the area 3b/1 border was identified by the greater intensity of immunostaining in layer IV of area 3b relative to that in area 1 (Fig. 8A, C). Immunoreactivity in the deeper layers of areas 4 and 1 began to appear clustered into vertically-oriented chains of puncta and radial streaks (Fig. 9C).

Between E155 and PND1.5, major changes in the distribution of immunostaining occurred which resulted in a pattern more closely resembling an adult-like one in all areas (Figs. 6, 10). The intensity of immunostaining, however, especially in superficial layers, was still less than in the adult (Figs. 6, 10). The principal changes from the pattern at E155 were a dramatic decrease in the intensity of immunostaining in layers IIIB and IV of areas 3, 1 and 2; the disappearance of the layer IV band in area 4, and an increase in the intensity of staining in layers I–IIIA of areas 4, 1 and 2 (Figs. 6, 10). In area 3, the staining intensity of layers I–IIIA was similar to that at E155. The staining intensity of layer IV in area 3 and of layers I and II in all areas was still less than in the adult, however (Figs. 6, 10B). In all areas, parallel chains of densely stained puncta were present in layer III, similar to those described in the adult (Fig. 10A, C). In areas 4, 1 and 2, long streaks of staining occurred in the middle layers and descended into the white matter in parallel with the radial fasciculi (Fig. 10A, C). Small numbers of immunoreactive, ovoid or round somata were present in all areas, although their numbers were greatest in area 4.

By PND 21, the intensity of immunostaining in layers I–IIIA of all areas had increased and was similar to that seen in the adult. In area 3, layers IV and VI also showed enhanced staining in comparison to younger ages, and appeared adult-like.

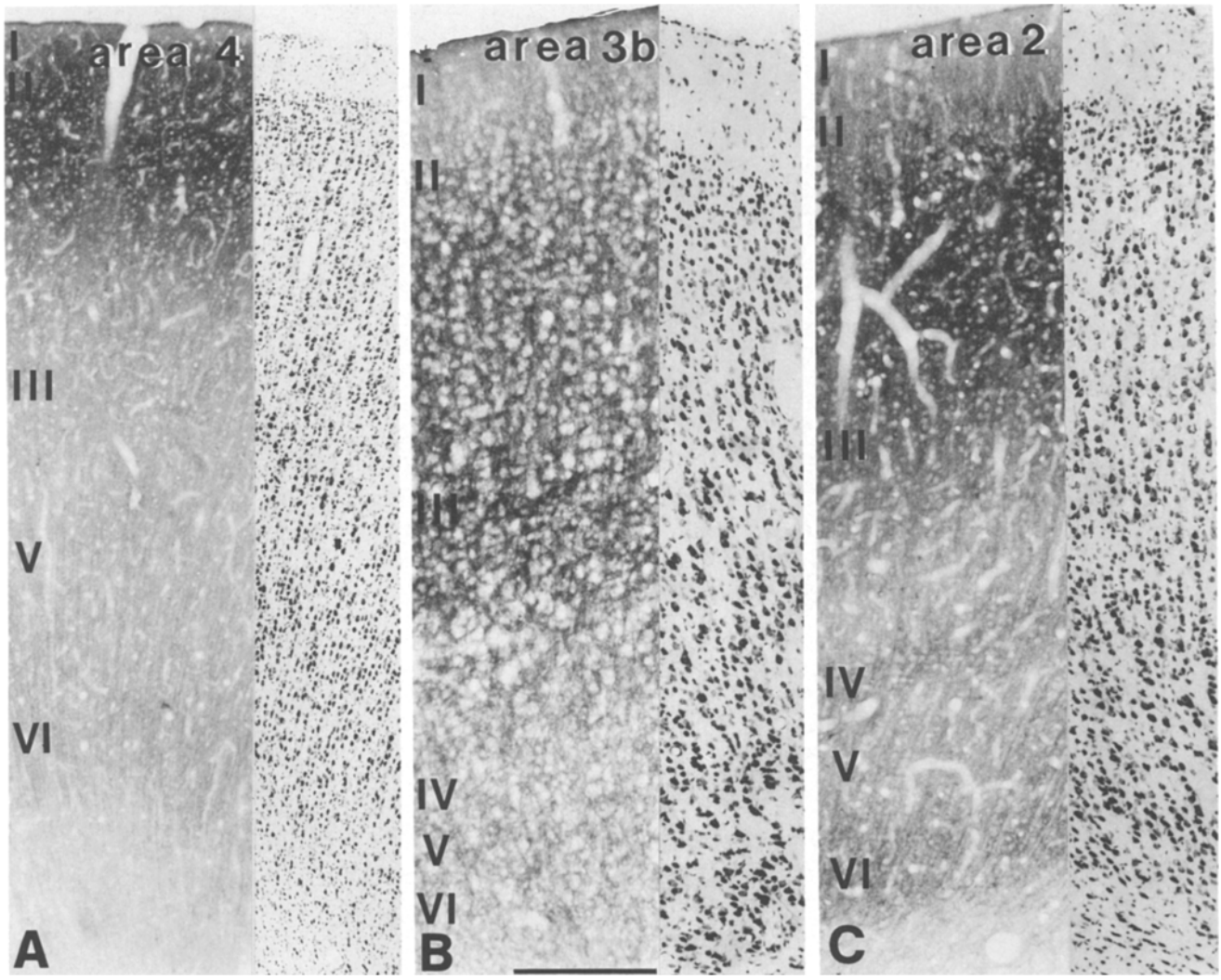

Fig. 10A–C. Pairs of photomicrographs from adjacent sections stained with thionin or for $GABA_A$ receptor immunoreactivity through area 4 (**A**), area 3b (**B**) or area 2 (**C**) from a PND 1.5 monkey. The distribution of immunostaining in all areas of the sensory-motor cortex changes between E155 and PND 1.5, and at PND 1.5 comes largely to resemble that of the adult. Bar: 500 μm (**A**) or 265 μm (**B, C**)

Discussion

In the present study, light microscopic, immunocytochemical techniques were used to examine the areal and laminar distribution of immunoreactive $GABA_A$ receptors in the adult monkey sensory-motor cortex, and to chart the developmental sequence by which such patterns of immunostaining in the adult become established during late fetal and early postnatal maturation of the sensory-motor cortex. The interpretation of these data depends critically on the reliability of the monoclonal antibody used to recognize the $GABA_A$ receptors.

Specificity of the monoclonal antibody and comparison with receptor autoradiography

The mouse monoclonal antibody used in this study has been previously characterized (Vitorica et al. 1988) and been shown in immunoblots to recognize selectively the 57000 Mr peptide subunit of the $GABA_A$ receptor/benzodiazepine receptor/Cl^- channel complex. A synthesis of data from several studies has suggested that this subunit contains the binding site for the GABA agonist ^{3}H-muscimol (Casalotti et al. 1986; Deng et al. 1986; Sieghart et al. 1987; Vitorica et al. 1988). The benzodiazepine binding site has been localized to a different peptide subunit than the one which binds ^{3}H-muscimol (Enna 1988). Immunocytochemical localization of $GABA_A$ receptors in various regions of rat brain by means of the same monoclonal antibody (de Blas et al. 1988) and in the monkey visual and motor cortex (Hendry et al. 1990; present results), is largely in accord with that revealed by binding of ^{3}H-muscimol and ^{3}H-flunitrazepam (rat: Palacios et al. 1981; Penney et al. 1981; Richards and Möhler 1984; McCabe and Wamsley 1986; monkey: Shaw and Cynader 1986; Rakic et al. 1988; Lidow et al. 1990). These data suggest that the epitope recognized by monoclonal antibody 62–3G1 is related selectively to the $GABA_A$ receptor component of the receptor complex (de Blas et al. 1988).

In the monkey somatic sensory cortex, the laminar

distribution of immunostained $GABA_A$ receptors matches more closely the laminar distribution of benzodiazepine receptors localized autoradiographically by ^{3}H-flunitrazepam binding than it does the distribution of receptor sites as identified by ^{3}H-muscimol binding (Lidow et al. 1990). It has been previously argued (de Blas et al. 1988) that the epitope recognized by the monoclonal antibody 62–3G1 is common to both the high-affinity and low-affinity forms of the $GABA_A$ receptor. The high-affinity receptor is thought to be functionally uncoupled to the benzodiazepine binding site and can be labeled with ^{3}H-muscimol (Palacios et al. 1981), while the low-affinity form is thought to be functionally coupled to the benzodiazepine site and can be labeled with ^{3}H-flunitrazepam (Tallman et al. 1978). Immunoprecipitation studies suggest, however, that both of the high- and low-affinity $GABA_A$ binding sites are physically coupled to the benzodiazepine binding site (Häring et al. 1985; Vitorica et al. 1988). Because the laminar distribution of $GABA_A$ receptor immunoreactivity follows more closely ^{3}H-flunitrazepam binding, it is likely to reflect the distribution of the low-affinity form of the $GABA_A$ receptor. It is the low-affinity form of the receptor which is thought to mediate physiological responses to GABA (Olsen et al. 1984).

In the present study, as in that on the monkey visual cortex (Hendry et al. 1990), immunoreactive staining outlined the surfaces of neuronal somata and often appeared in the neuropil in patterns such as linear streaks and chains of puncta, suggestive of outlined dendrites or chains of terminal boutons on which the receptors are probably being localized. In the case of the intracellular immunostaining observed in the present study, it is unlikely that the epitopic sites stained represent functional receptors. A previous immunocytochemical study of $GABA_A$ receptor distribution in the cerebellum (utilizing a different monoclonal antibody to the $GABA_A$ receptor than the one used here) also revealed an intracellular accumulation of reaction product in some cells, and electron microscopic examination localized the immunoreactivity to the membranes of the endoplasmic reticulum and Golgi apparatus (Somogyi et al. 1989). The presence of such intracellularly located epitopic regions may be indicative of various stages of synthesis and assembly of the receptors (Sweetnam and Tallman 1986; Kuriyami and Taguchi 1987). It is clear, however, that not all cell types which are thought to possess $GABA_A$ receptors exhibit the intracellularly distributed reaction product. For example, the somata of pyramidal cells in the human hippocampal formation (Houser et al. 1988) and in the monkey cerebral cortex (Hendry et al. 1990; present study) are not immunoreactive, which may be indicative of differences in the accessibility of the antibodies or in the rate of turnover of receptors between different cell classes.

GABA-mediated transmission in the sensory-motor cortex

In adult monkey somatic sensory cortex, there is no clear correlation between layers with a high density of receptor staining and those with a high density of GABA cells. GABA-immunoreactive cells and GAD-immunoreactive puncta (presumptive terminals) are concentrated in layers which receive the major terminations of thalamocortical axons (Hendry and Jones 1981; Houser et al. 1983; Hendry et al. 1987b). These layers correspond to layers IIIB and IV of areas 3a and 3b and to layer III of areas 1 and 2 (Jones 1975b; Jones and Burton 1976). Although layer IV throughout all areas of SI shows enhanced receptor staining, the staining is considerably less than that of layers I–IIIA and, in layer IIIB, receptor staining is weak. In SI, there is a clear difference in comparison with the visual cortex in which studies of $GABA_A$ receptor distribution by immunocytochemistry (Hendry et al. 1990) and autoradiography (Rakic et al. 1988; Shaw and Cynader 1986) show a good correlation between layers with a high density of receptor staining or binding and those with a high density of GABA terminals (Fitzpatrick et al.1987) and the presence of thalamocortical axon terminals. Despite the lack of a clear correlation between $GABA_A$ receptor density and layers of thalamocortical terminations, in SI, GABA cell density tends to be highest in the thalamocortical recipient layers, so $GABA_A$ receptor mediated inhibition may still be influential at the early stages of somatic sensory information processing, as in the visual cortex (Sillito 1984; Ferster 1986, 1987, 1988).

In the motor cortex, GABAergic cells and puncta are densest in layers I–IIIA (Hendry and Jones 1981; Houser et al. 1983; Hendry et al. 1987b). Although there is a good correlation between the density of $GABA_A$ receptor staining and GABA cell distribution, there is no obvious correlation between these and the distribution of thalamocortical axon terminals. Thalamocortical axons terminate mainly in the deeper half of layer III (Jones 1975a; Jones and Burton 1976) in which receptor immunoreactivity is weak. The seemingly sparse distribution of GABAergic cells and $GABA_A$ receptors in the deeper half of layer III, which receives the main terminations of thalamocortical axons in motor cortex, in comparison to somatic sensory or visual cortex, may simply reflect differences between koniocortical and agranular areas in the degree to which some thalamorecipient cell types are compacted into a recognizable layer. It is thought that the agranular nature of motor cortex represents the dispersion of cell types which in the fetal cortex form a compacted layer IV (Ramón y Cajal 1900; Marin-Padilla 1970; unpublished observations). This is paralleled by the appearance of a transient zone of $GABA_A$ receptor staining in association with the transient layer IV of area 4.

In layers V and VI of the motor cortex, the intensity of $GABA_A$ receptor immunoreactivity is quantitatively greater than that in the middle layers, suggesting a greater concentration of receptors in these layers. This observation differs from that obtained in quantitative radioligand binding studies (Lidow et al. 1990), which reveal a rather uniform distribution of both ^{3}H-muscimol and ^{3}H-flunitrazepam binding sites across layers IIIB–VI. This discrepancy most likely reflects the lower resolution inherent in autoradiographic methods compared with immunocytochemical methods. A similar conclusion was reached in a study of monkey visual

cortex in which $GABA_A$ receptor immunoreactivity revealed a greater degree of sub-laminar organization (Hendry et al. 1990) than could be revealed by $GABA_A$ or benzodiazepine receptor autoradiography (Rakic et al. 1988; Hendry et al. 1990). Although the density of GABAergic cells is much lower in deeper layers than in superficial ones (Hendry et al. 1987b), studies utilizing the uptake of ^{3}H–GABA and those utilizing GABA and calcium-binding protein immunocytochemistry have shown that GABAergic cells of superficial layers provide a major input to deeper layers (Somogyi et al. 1981; DeFelipe et al. 1985, 1989; Hendry et al. 1989). It is possible that the increased $GABA_A$ receptor staining in deeper layers correlates with the terminals of such projections. The streaklike pattern and fasciculation of receptor immunostaining in several of the areas may reflect the bundles characteristic of the axons of these cells (DeFelipe et al. 1989; Hendry et al. 1989).

Layers II–IIIA show the densest $GABA_A$ receptor immunoreactivity in all areas of the sensory-motor cortex. These layers furnish and receive the major corticocortical connections (Jones and Wise 1977; Jones et al. 1978; Jones 1986), and it has been shown that such projections terminate as multiple foci, forming a striplike configuration (Jones et al. 1975, 1978; Goldman and Nauta 1977). These anatomical data may represent the underlying basis for the intermittent, patch-like distribution of ^{14}[C]-2-D–deoxyglucose (2–DG) labeling following repeated somatic stimulation of a restricted part of the periphery (Durham and Woolsey 1985; Juliano et al. 1981; Hand 1982; Juliano and Whitsel 1985; Juliano et al. 1989). Juliano et al. (1989) have shown that the characteristic 2–DG patches observed following cutaneous stimulation are dramatically altered if bicuculline methiodide, a competitive $GABA_A$ receptor antagonist, is applied topically to the somatic sensory cortex prior to 2–DG administration. Such patches tend to widen and fuse, and become especially prominent in the supragranular layers (Juliano et al. 1989). The high intensity of receptor immunostaining in the supragranular layers suggests high numbers of receptors in these layers, which may therefore underlie the particular sensitivity of supragranular neurons to BIC, and may suggest a critical role of $GABA_A$ receptor mediated inhibition in the preservation of the topography and/or functional properties established by such corticocortical projections (Juliano et al. 1989).

$GABA_A$ receptor immunostaining in the subplate of the fetal cortex

The presence of $GABA_A$ receptor immunoreactivity in the subplate zone contributes to a growing body of data which suggests that this transient, developmentally regulated zone may be an early locus of synaptic circuitry prior to and during the establishment of connectivity in the overlying cortical layers.

It has been proposed that the constituent cells of the subplate zone serve as temporary targets for ingrowing corticopetal fibers (Shatz et al. 1988). This view has as its basis several sets of observations. It is well known that ingrowing thalamocortical and callosal axons undergo a protracted wait in the subplate zone prior to subsequent ingrowth into the cortex (Lund and Mustari 1977; Rakic 1977; Wise et al. 1977; Innocenti 1981; Shatz and Luskin 1986; Killackey and Chalupa 1986; reviewed in Rakic 1988). Ultrastructural studies have identified the marginal and subplate zones as the first synapse-rich strata to emerge in the developing cortex (Kostović et al. 1973; Molliver et al. 1973; Kostović and Molliver 1974; Cragg 1975; Wolff 1976; Blue and Parnavelas 1983; Chun et al. 1987; Valverde and Facal-Valverde 1988), and the subplate zone in fetal cats is immunoreactive for Synapsin I (Chun and Shatz 1988), a molecule associated with synaptic vesicles (Bloom et al. 1979; Mathew et al. 1981; Llinás et al. 1985; De Camilli and Greengard 1986). Many subplate neurons during development are immunoreactive for GABA, for neuropeptides or for both (Chun et al. 1987; Huntley et al. 1987, 1988; Wahle and Meyer 1987; reviewed in Shatz et al. 1988), and in cats have been shown to make local and interhemispheric connections (Chun et al. 1987; unpublished observations in Chun and Shatz 1989a). These data support the view of subplate neurons being synaptically active, and, as such, may be subject to $GABA_A$ receptor-mediated inhibition.

In the present study, $GABA_A$ receptor immunoreactivity was always much more diffuse in the subplate than in the overlying cortical layers. The diffuse quality may reflect the lower cell- and synaptic density of the subplate compared to overlying layers (Zecevic et al. 1989). The decline in $GABA_A$ receptor immunostaining in the subplate with increasing age is probably contemporaneous with the gradual elimination of the subplate zone itself. It has been shown, however, that some subplate neurons survive into adulthood as typical interstitial cells of the white matter in cats (Chun and Shatz 1989b), and many such cells in adult monkeys show immunoreactivity for GABA and for one or more neuropeptides, and appear to participate in cortical circuitry (Hendry et al. 1984; Jones et al. 1988).

$GABA_A$ receptor immunoreactivity within the cell-dense layers of the fetal monkey sensory-motor cortex also gradually undergoes changes in intensity over time. It is unlikely that species differences account for the changes observed in the patterns of immunostaining. No species differences were observed in the patterns of immunostaining in the adult animals and at the developmental ages (for example, E121 and E125) at which two species of macaques, each perfused with different concentrations of fixatives, could be compared. It is difficult, however, to correlate the changes seen in staining intensity from one age to the next with changes in numbers of receptors. Quantitative autoradiographic studies in developing cat visual cortex reveal a steady increase and eventual overshoot in the number of ^{3}H-muscimol binding sites, which gradually decline to adult-like levels (Shaw et al. 1984). Therefore, the gradual increase in intensity of receptor immunostaining seen over time is likely to reflect increases in the concentrations of $GABA_A$ receptors. It is clear that relative receptor distribution by

layers gradually acquires an adult-like pattern over time, temporally coincident with the ingrowth and establishment of certain sets of connections (Killackey and Chalupa 1986; Chalupa and Killackey 1989). As callosal axons, and other ingrowing fibers, refine their projections to an adult-like pattern, $GABA_A$ receptors may be induced and their distribution modified. The ingrowth of geniculocortical fibers into layer IV of cat visual cortex is correlated, for example, with the transient appearance of nicotinic receptors in this layer (Prusky et al. 1988).

Functionally, the relatively early appearance of adult-like distributions of $GABA_A$ receptor immunoreactivity and of GABA-immunoreactive neurons (Huntley et al. 1987; unpublished observations) in the monkey sensory-motor cortex may signify that well-developed inhibitory circuitry is acquired early, and may be partly responsible for the early acquisition of an adult-like capacity for tactile discrimination observed in infant macaques (Carlson 1984). Activity dependent regulation of $GABA_A$ receptor distribution, as demonstrated in the visual cortex of monkeys (Hendry et al. 1990), may play a key role in the establishment of sensory-motor maps during this period and the plasticity of representational maps in adulthood (Rasmusson 1982; Kelahan and Doetsch 1984; Merzenich et al. 1984; Wall and Cusick 1984; Merzenich et al. 1988).

Acknowledgements. Supported by grant no. NS 21377 from the National Institutes of Health, United States Public Health Service, by the NIMH Center for Neuroscience and Schizophrenia, MH44188, and by a National Institute of Mental Health predoctoral fellowship to G.W.H. We thank Drs. A.E. Hendrickson, H.P. Killackey, D.L. Lewis and L.M. Chalupa for kindly providing some brains.

References

Alloway KD, Burton H (1986) Bicuculline-induced alterations in neuronal responses to controlled tactile stimuli in the second somatosensory cortex of the cat: a microiontophoretic study. Somatosens Res 3:197–211

Barnard EA, Darlison MG, Seeburg P (1987) Molecular biology of the $GABA_A$ receptor: the receptor/channel superfamily. Trends Neurosci 10:502–509

Bloom FE, Ueda T, Battenberg E, Greengard P (1979) Immunocytochemical localization in synapses of protein I an endogenous substrate for protein kinases in mammalian brain. Proc Natl Acad Sci USA 76:5982–5986

Blue ME, Parnavelas JG (1983) The formation and maturation of synapses in the visual cortex of rat. II. Quantitative analysis. J Neurocytol 12:697–712

Bowery NG, Price GW, Hudson AL, Hill DR, Wilkin GP, Turnbull MJ (1984) GABA receptor multiplicity: visualization of different receptor types in the mammalian CNS. Neuropharmacol 23:219–231

Cajal S Ramón y (1900) Estudios sobre la corteza cerebral humana. II. Corteza motriz (conclusión). Rev Trimestr Microgr Madrid 5:1–11

Carlson M (1984) Development of tactile discrimination capacity in Macaca mulatta. I. Normal infants. Dev Brain Res 16:69–82

Casalotti SO, Stephenson FA, Barnard EA (1986) Separate subunits for agonist and benzodiazepine binding in the $GABA_A$ receptor oligomer. J Biol Chem 261:15 013–15 016

Chalupa LM, Killackey HP (1987) Double-labeled neurons in primary somatosensory cortex (area 3b) of the fetal rhesus monkey. Soc Neurosci Abstr 13:76

Chalupa LM, Killackey HP (1989) Process elimination underlies ontogenetic change in the distribution of callosal projection neurons in the postcentral gyrus of the fetal rhesus monkey. Proc Natl Acad Sci USA 86:1076–1079

Chudler EH, Pretel S, Kenshalo Jr. DR (1988) Distribution of GAD-immunoreactive neurons in the first (SI) and second (SII) somatosensory cortex of the monkey. Brain Res 456:57–63

Chun JJM, Shatz CJ (1988) Redistribution of synaptic vesicle antigens is correlated with the disappearance of a transient synaptic zone in the developing cerebral cortex. Neuron 1:297–310

Chun JJM, Shatz CJ (1989a) The earliest-generated neurons of the cat cerebral cortex: characterization by MAP2 and neurotransmitter immunohistochemistry during fetal life. J Neurosci 9:1648–1667

Chun JJM, Shatz CJ (1989b) Interstitial cells of the adult neocortical white matter are the remnant of the early-generated subplate neuron population. J Comp Neurol 282:555–569

Chun JJM, Nakamura MJ, Shatz CJ (1987) Transient cells of the developing mammalian telencephalon are peptide immunoreactive neurons. Nature 325:617–620

Connors BW, Malenka RC, Silva LR (1988) Two inhibitory postsynaptic potentials and $GABA_A$ and $GABA_B$ receptor-mediated responses in neocortex of rat and cat. J Physiol (London) 406:443–468

Cragg BG (1975) The development of synapses in the visual system of the cat. J Comp Neurol 160:147–166

Creutzfeldt OD, Ito M (1968) Functional synaptic organisation of primary visual cortex neurones in the cat. Exp Brain Res 6:324–352

de Blas AL, Vitorica J, Friedrich P (1988) Localization of the $GABA_A$ receptor in the rat brain with a monoclonal antibody to the 57 000 M_r peptide of the $GABA_A$ receptor/benzodiazepine receptor/Cl^- channel complex. J Neurosci 8:602–614

De Camilli P, Greengard P (1986) Synapsin I: a synaptic vesicle-associated neuronal phosphoprotein. Biochem Pharmacol 35:4349–4357

DeFelipe J, Jones EG (1985) Vertical organization of γ-aminobutyric acid-accumulating intrinsic neuronal systems in monkey cerebral cortex. J Neurosci 5:3246–3260

DeFelipe J, Hendry SHC, Jones EG (1986) A correlative electron microscopic study of basket cells and large GABAergic neurons in the monkey sensory-motor cortex. Neuroscience 17:991–1009

DeFelipe J, Hendry SHC, Jones EG (1989) Synapses of double bouquet cells in monkey cerebral cortex visualized by calbindin immunoreactivity. Brain Res 503:49–54

DeFelipe J, Hendry SHC, Jones EG, Schmechel D (1985) Variability in the terminations of GABAergic chandelier cell axons on initial segments of pyramidal cell axons in the monkey sensory-motor cortex. J Comp Neurol 231:364–384

Deng L, Ransom RW, Olsen RW (1986) (^{3}H)muscimol photolabels the GABA receptor binding site on a peptide subunit distinct from that labeled with benzodiazepines. Biochem Biophys Res Commun 138:1308–1314

Durham D, Woolsey TA (1985) Functional organization in cortical barrels of normal and vibrissae-damaged mice: a (^{3}H) 2-deoxyglucose study. J Comp Neurol 235:97–110

Dykes RW, Landry P, Metherate R, Hicks TP (1984) Functional role of GABA in cat primary somatosensory cortex: shaping receptive fields of cortical neurons. J Neurophysiol 52:1066–1093

Enna SJ, (1988) GABA–A receptors. In: Squires RF (ed) GABA and benzodiazepine receptors, Vol. 1. CRC Press Inc, pp 91–106

Ferster D (1986) Orientation selectivity of synaptic potentials in neurons of cat primary visual cortex. J Neurosci 6:1284–1301

Ferster D (1987) Origin of orientation-selective EPSPs in simple cells of cat visual cortex. J Neurosci 7:1780–1791

Ferster D (1988) Spatially opponent excitation and inhibition in simple cells of the cat visual cortex. J Neurosci 8:1172–1180

Fitzpatrick D, Lund JS, Schmechel DE, Towles AC (1987) Distribution of GABAergic neurons and axon terminals in the macaque striate cortex. J Comp Neurol 264:73–91

Goldman PS, Nauta WHJ (1977) Columnar distribution of cortico-cortical fibers in the frontal association, limbic and motor cortex of the developing rhesus monkey. Brain Res 122:393–414

Hand PJ (1982) Plasticity of the rat cortical barrel system. In: Strick PL, Morrison AR (eds) Changing concepts of the nervous system. Academic, New York, pp 49–68

Häring P, Stähli C, Schoch P, Takács B, Staehelin T, Möhler H (1985) Monoclonal antibodies reveal structural homogeneity of γ-aminobutyric acid/benzodiazepine receptors in different brain areas. Proc Natl Acad Sci USA 82:4837–4841

Hendry SHC, Jones EG (1981) Sizes and distributions of intrinsic neurons incorporating tritiated GABA in monkey sensory-motor cortex. J Neurosci 4:390–408

Hendry SHC, Jones EG, Emson PC (1984) Morphology, distribution and synaptic relations of somatostatin and neuropeptide Y immunoreactive neurons in rat and monkey neocortex. J Neurosci 5:2254–2268

Hendry SHC, Houser CR, Jones EG, Vaughn JE (1983) Synaptic organization of immunocytochemically identified GABA neurons in the monkey sensory-motor cortex. J Neurocytol 12:639–660

Hendry SHC, Jones EG, Killackey HP, Chalupa LM (1987a) Choline acetyltransferase-immunoreactive neurons in fetal monkey cerebral cortex. Dev Brain Res 37:313–317

Hendry SHC, Schwark HD, Jones EG, Yan J (1987b) Numbers and proportions of GABA immunoreactive neurons in different areas of monkey cerebral cortex. J Neurosci 7:1503–1520

Hendry SHC, Jones EG, Emson PC, Lawson DEM, Heizmann CW, Streit P (1989) Two classes of cortical GABA neurons defined by differential calcium binding protein immunoreactivities. Exp Brain Res 76:467–472

Hendry SHC, Fuchs J, de Blas AL, Jones EG (1990) Distribution and plasticity of immunocytochemically localized $GABA_A$ receptors in adult monkey visual cortex. J Neurosci 10:2438–2450

Hicks TP, Dykes RW (1983) Receptive field size for certain neurons in primary somatosensory cortex is determined by GABA-mediated intracortical inhibition. Brain Res 274:160–164

Houser CR, Hendry SHC, Jones EG, Vaughn JE (1983) Morphological diversity of immunocytochemically identified GABA neurons in the monkey sensory-motor cortex. J Neurocytol 12:617–638

Houser CR, Vaughn JE, Hendry SHC, Jones EG, Peters A (1984) GABA neurons in the cerebral cortex. In: Jones EG, Peters P (eds) Cerebral cortex, Vol 2. Plenum Press, New York, pp 63–89

Houser CR, Olsen RW, Richards JG, Möhler H (1988) Immunohistochemical localization of benzodiazepine/$GABA_A$ receptors in the human hippocampal formation. J Neurosci 8:1370–1383

Huntley GW, Jones EG (1990) Cajal-Retzius neurons in developing monkey neocortex show immunoreactivity for calcium binding proteins. J Neurocytol 19:200–212

Huntley GW, Hendry SHC, Jones EG, Chalupa LM, Killackey HP (1987) GABA, neuropeptide and ChaT expression in neurons of the fetal monkey sensory-motor cortex. Soc Neurosci Abstr 13:76

Huntley GW, Hendry SHC, Killackey HP, Chalupa LM, Jones EG (1988) Temporal sequence of neurotransmitter expression by developing neurons of fetal monkey visual cortex. Dev Brain Res 43:69–96

Innocenti GM (1981) Growth and reshaping of axons in the establishment of visual callosal connections. Science 212:824–827

Jones EG (1975a) Varieties and distribution of non-pyramidal cells in the somatic sensory cortex of the squirrel monkey. J Comp Neurol 160:167–204

Jones EG (1975b) Lamination and differential distribution of thalamic afferents in the sensory-motor cortex of the squirrel monkey. J Comp Neurol 160:167–204

Jones EG (1986) Connectivity of the primate sensory-motor cortex. In: Jones EG, Peters A (eds) Cerebral cortex, Vol 5. Plenum, New York, pp 113–183

Jones EG, Burton H (1976) Areal differences in the laminar distribution of thalamic afferents in cortical fields of the insular parietal and temporal regions of primates. J Comp Neurol 168:197–247

Jones EG, Wise SP (1977) Size, laminar and columnar distribution of efferent cells in the sensory-motor cortex of monkeys. J Comp Neurol 175:391–438

Jones EG, Burton H, Porter R (1975) Commissural and corticocortical "columns" in the somatic sensory cortex of primates. Science 190:572–574

Jones EG, Coulter JD, Hendry SHC (1978) Intracortical connectivity of architectonic fields in the somatic sensory, motor and parietal cortex of monkeys. J Comp Neurol 181:291–347

Jones EG, DeFelipe J, Hendry SHC, Maggio JE (1988) A study of tachykinin immunoreactive neurons in monkey cerebral cortex. J Neurosci 8:1206–1225

Juliano SL, Whitsel BL (1985) Metabolic labeling associated with index finger stimulation in monkey SI: between animal variability. Brain Res 342–251

Juliano SL, Hand PJ, Whitsel BL (1981) Patterns of increased metabolic activity in somatosensory cortex of monkeys *(Macaca fascicularis)* subjected to controlled cutaneous stimulation: a 2-deoxyglucose study. J Neurophysiol 46:1260–1284

Juliano SL, Whitsel BL, Tommerdahl M, Cheema SS (1989) Determinants of patchy metabolic labeling in the somatosensory cortex of cats: a possible role for intrinsic inhibitory circuitry. J Neurosci 9:1–12

Kelahan AM, Doetsch GS (1984) Time-dependent changes in the functional organization of somatosensory cerebral cortex following digit amputation in adult raccoons. Somatosens Res 2:49–81

Kelly JS, Krnjević K, Morris ME, Yim GKW (1969) Anionic permeability of cortical neurones. Exp Brain Res 7:11–31

Killackey HP, Chalupa LM (1986) Ontogenetic change in the distribution of callosal projection neurons in the postcentral gyrus of the fetal rhesus monkey. J Comp Neurol 244:331–348

Kostović I, Molliver ME (1974) A new interpretation of the laminar development of cerebral cortex: synaptogenesis in different layers of neopallium in the human fetus. Anat Rec 178:395 (Abstr.)

Kostović I, Molliver ME, Van der Loos H (1973) The laminar distribution of synapses in neocortex of fetal dog. Anat Rec 175:362 (Abstr.)

Kuriyama K, Taguchi J (1987) Glycoprotein as a constituent of purified gamma-aminobutyric acid/benzodiazepine receptor complex: structures and physiological roles of its carbohydrate chain. J Neurochem 48:1897–1903

Lidow MS, Goldman-Rakic PS, Gallager DW, Geschwind DH, Rakic P (1990) Distribution of major neurotransmitter receptors in the motor and somatosensory cortex of the rhesus monkey. Neuroscience 32:609–627

Llinás R, McGuiness TL, Leonard CS, Sugimori M, Greengard P (1985) Intraterminal injection of synapsin I or calcium/calmodulin-dependent protein kinase II alters neurotransmitter release at the squid giant synapse. Proc Natl Acad Sci USA 82:3035–3039

Lund RD, Mustari MJ (1977) Development of the geniculocortical pathway in rats. J Comp Neurol 173:289–306

Marin-Padilla M (1970) Prenatal and early postnatal ontogenesis of the human motor cortex: a Golgi study. I. The sequential development of the cortical layers. Brain Res 23:167–183

Matthew WD, Tsavaler L, Reichardt LF (1981) Identification of a synaptic vesicle-specific membrane protein with a wide distribution in neuronal neurosecretory tissue. J Cell Biol 91:257–269

McCabe RT, Wamsley JK (1986) Autoradiographic localization of subcomponents of the macromolecular GABA receptor complex. Life Sci 39:1937–1946

Merzenich MM, Nelson RJ, Stryker MP, Cynader MS, Schoppmann A, Zook JM (1984) Somatosensory cortical map changes following digit amputation in adult monkeys. J Comp Neurol 224:591–605

Merzenich MM, Recanzone G, Jenkins WM, Allard T, Nudo RJ (1988) Cortical representational plasticity. In: Changeux JP,

Konishi M (eds) The neural and molecular basis of learning. John Wiley and Sons, Chichester, England
Molliver ME, Kostović I, Van der Loos H (1973) The development of synapses in cerebral cortex of the human fetus. Brain Res 50:403–407
Olsen RW, Snowhill EW, Wamsley JD (1984) Autoradiographic localization of low affinity GABA receptors with ^{3}H-bicuculline methochloride. Eur J Pharmacol 99:245–247
Palacios JM, Wamsley JK, Kuhar MJ (1981) High affinity GABA receptors: Autoradiographic localization. Brain Res 222:285–307
Penney JB, Pan HS, Young AB, Frey KA, Dauth GW (1981) Quantitative autoradiography of (^{3}H)-muscimol binding in rat brain. Science 214:1036–1038
Prusky GT, Arbuckle JM, Cynader MS (1988) Transient concordant distributions of nicotinic receptors and acetylcholinesterase activity in infant rat visual cortex. Dev Brain Res 39:154–159
Rakic P (1977) Prenatal development of the visual system in rhesus monkey. Philos Trans R Soc London Ser B 278:245–260
Rakic P (1988) Specification of cerebral cortical areas. Science 241:170–176
Rakic P, Goldman-Rakic PS, Gallagher D (1988) Quantitative autoradiography of major neurotransmitter receptors in the monkey striate and extrastriate cortex. J Neurosci 8:3670–3690
Ramoa AS, Paradiso MA, Freeman RD (1988) Blockade of intracortical inhibition in kitten striate cortex: effects on receptive field properties and associated loss of ocular dominance plasticity. Exp Brain Res 73:285–298
Rasmusson DD (1982) Reorganization of raccoon somatosensory cortex following removal of the fifth digit. J Comp Neurol 205:313–326
Richards RF, Möhler H (1984) Benzodiazepine receptors Neuropharmacology 23:233–242
Shatz CJ, Luskin MB (1986) The relationship between the geniculocortical afferents and their cortical target cells during development of the cat's primary visual cortex. J Neurosci 6:3655–3668
Shatz CJ, Chun JJM, Luskin MB (1988) The role of the subplate in the development of the mammalian telencephalon. In: Peters A, Jones EG (eds) The cerebral cortex, Vol 7. Plenum, New York, pp 35–58
Shaw C, Cynader M (1986) Laminar distribution of receptors in monkey *(Macaca fascicularis)* geniculostriate system. J Comp Neurol 248:301–312
Shaw C, Needler MC, Cynader M (1984) Ontogenesis of muscimol binding sites in cat visual cortex. Brain Res Bull 13:331–334
Sieghart W, Eichinger A, Richards JG, Möhler H (1987) Photoaffinity labeling of benzodiazepine receptor proteins with the partial inverse agonist (^{3}H)Ro15–4513: a biochemical and autoradiographic study. J Neurochem 48:46–52
Sillito AM (1984) Functional considerations of the operation of GABAergic inhibitory processes in the visual cortex. In: Jones EG, Peters A (eds) Cerebral cortex, Vol 2. Plenum, New York, pp 91–117
Somogyi P, Cowey A, Halasz N, Freund TF (1981) Vertical organization of neurones accumulating ^{3}H–GABA in visual cortex of rhesus monkey. Nature 294:761–763
Somogyi P, Takagi H, Richards JG, Möhler H (1989) Subcellular localization of benzodiazepine/$GABA_A$ receptors in the cerebellum of rat,cat and monkey using monoclonal antibodies. J Neurosci 9:2197–2209
Sweetman P, Tallman JF (1986) Regional differences in brain benzodiazepine receptor carbohydrates. Mol Pharmacol 29:299–306
Tallman JF, Thomas JW, Gallager DW (1978) GABAergic modulation of benzodiazepine binding site sensitivity. Nature 274:383–385
Tsumoto T, Eckhart W, Creutzfeldt OD (1979) Modification of orientation sensitivity of cat visual cortex neurons by removal of GABA-mediated inhibition. Exp Brain Res 34:351–363
Valverde F, Facal-Valverde MV (1988) Postnatal development of interstitial (subplate) cells in the white matter of the temporal cortex of kittens: a correlated Golgi and electron microscopic study. J Comp Neurol 269:168–192
Vitorica J, Park D, Chin G, de Blas AL (1988) Monoclonal antibodies and conventional antisera to the $GABA_A$ receptor/benzodiazepine/Cl^- channel complex. J Neurosci 8:615–622
Wahle P, Meyer G (1987) Morphology and quantitative changes of transient NPY-ir neuronal populations during early postnatal development of the cat visual cortex. J Comp Neurol 261:165–192
Wall JT, Cusick CG (1984) Cutaneous responsiveness in primary somatosensory (SI) hindpaw cortex before and after partial hindpaw deafferentation in adults rats. J Neurosci 4:1499–1515
Wise SP, Hendry SHC, Jones EG (1977) Prenatal development of sensorimotor cortical projections in cats. Brain Res 138:538–544
Wolff JR (1976) Quantitative analysis of topography and development of synapses in visual cortex. Exp Brain Res Suppl 1:259–263
Woolf NJ, Butcher LL (1981) Cholinergic neurons in the caudate-putamen complex proper are intrinsically organized: a combined evans blue and acetylcholinesterase analysis. Brain Res Bull 7:487–507
Wong-Riley MTT (1979) Changes in the visual system of monocularly sutured or enucleated cats demonstrable with cytochrome oxidase histochemistry. Brain Res 171:11–28
Zecevic N, Bourgeois J-P, Rakic P (1989) Changes in synaptic density in motor cortex of rhesus monkey during fetal and postnatal life. Dev Brain Res 50:11–32